

Anchorage of mature conifers: resistive turning moment, root–soil plate geometry and root growth orientation

TOR LUNDSTRÖM,^{1,2} TOBIAS JONAS,¹ VERONIKA STÖCKLI¹ and WALTER AMMANN¹

¹ WSL, Swiss Federal Institute for Snow and Avalanche Research SLF, CH-7260 Davos, Switzerland

² Corresponding author (t.lundstroem@slf.ch)

Received September 30, 2006; accepted December 12, 2006; published online June 1, 2007

Summary Eighty-four mature Norway spruce (*Picea abies* L. Karst), silver fir (*Abies alba* Mill) and Scots pine (*Pinus sylvestris* L.) trees were winched over to determine the maximum resistive turning moment (M_a) of the root–soil system, the root–soil plate geometry, the azimuthal orientation of root growth, and the occurrence of root rot. The calculation of M_a , based on digital image tracking of stem deflection, accounted not only for the force application and its changing geometry, but also for the weight of the overhanging tree, representing up to 42% of M_a . Root rot reduced M_a significantly and was detected in 25% of the Norway spruce and 5% of the silver fir trees. Excluding trees with root rot, differences in M_a between species were small and insignificant. About 75% of the variance in M_a could be explained by one of the four variables—tree mass, stem mass, stem diameter at breast height squared times tree height, and stem diameter at breast height squared. Among the seven allometric variables assessed above ground, stem diameter at breast height best described the root–soil plate dimensions, but the correlations were weak and the differences between species were insignificant. The shape of the root–soil plate was well described by a depth-dependent taper model with an elliptical cross section. Roots displayed a preferred azimuthal orientation of growth in the axis of prevailing winds, and the direction of frequent weak winds matched the orientation of growth better than that of rare strong winds. The lack of difference in anchorage parameters among species probably reflects the similar belowground growth conditions of the mature trees.

Keywords: allometry, biomechanics, natural hazards, preferential growth, tree structure, winching experiment.

Introduction

The mechanical stability of a forest is challenged by strong winds (e.g., Schiessler et al. 1997). The maximum resistance to turning moment of the root–soil system, denoted by the anchorage strength (M_a), is typically the weakest mechanical link for shallow-rooted trees subjected to strong winds (Papesch et al. 1997, Brassel and Brändli 1999). Values of M_a are commonly obtained in winching experiments (e.g., Coutts 1986, Milne and Blackburn 1989, Crook and Ennos 1996).

The moment effectively applied to the root–soil system in such experiments includes the moment due to the winching force and to the weight of the leaning tree. Both factors depend on the position of the stem, which is constantly changing during the winching test.

Almost 40 different series of winching tests have been performed since the sixties (e.g., Fraser 1962, Nicoll et al. 2005). For these tests, a variety of approaches were used to account for changes in the position of the stem, and thus in test geometry, for the calculation of M_a . Overhanging tree weight can amount to between 20 (Peltola 1995, Gardiner et al. 2000) and 70% of M_a (Coutts 1986). Our analysis showed that a change in the geometry of the applied winching force also needs to be considered in the calculation of M_a . When analyzing anchorage mechanics, it is important to know the effective applied and reacting turning moment of the root–soil system because the root–soil system is considered an isolated structural element, or an isolated group of elements, when applying the finite element methods (FEMs). The FEMs are increasingly being applied in the analysis of tree mechanics (Fourcaud et al. 2003a, 2003b, Dupuy et al. 2005, Yang et al. 2005, Jonsson et al. 2006).

The value of M_a is positively related to the sum of root cross sections at one fixed horizontal distance (e.g., at 0.5 m) from the center line of the stem (Crook and Ennos 1996, Bolenikus 2001), the mass of the woody roots and, to some extent, the size of the root–soil plate and the rooting depth (e.g., Mattheck et al. 1993, Wessolly and Erb 1998, Bolenikus 2001, Meunier et al. 2002). Higher M_a values are found for trees on the edge of a stand than within the stand (Cucchi et al. 2004), and for trees with interlocked root systems (Coutts 1983). The value of M_a depends on soil conditions (Fraser and Gardiner 1967, Moore 2000). Further, M_a is strongly related to tree parameters aboveground (e.g., tree mass, stem mass, stem diameter at breast height and tree height) (e.g., Peltola et al. 2000, Cucchi et al. 2004, Stokes et al. 2005, Nicoll et al. 2006). Winching tests have mostly been conducted on small and young trees because they are usually considered more vulnerable to wind than large trees. Consequently, values of M_a , in combination with below- and aboveground tree parameters, have been determined almost exclusively for small trees.

The size and shape of the overturned root–soil plate indicate

how roots are anchored in the soil and must be known when modeling the mechanics of the root–soil system (Coutts 1983, 1986, Blackwell et al. 1990, Danjon et al. 2005). Various idealized shapes have been used to describe the root–soil plate; however, we were unable to find a three-dimensional description based on experimental data.

Excavations of the root system of young trees show preferential root growth in the direction of the prevailing winds (Stokes et al. 1995, Nicoll and Ray 1996, Mickovski and Ennos 2003a, Danjon et al. 2005). The degree of such adaptive growth depends not only on the magnitude and frequency of the prevailing wind, but also on the species and the growth conditions (Nicoll et al. 1995, Coutts et al. 1999). It is possible that mature conifers, like young ones, display a prevailing azimuthal direction of root growth depending on wind load, but, to our knowledge, this has never been demonstrated.

To improve the design of mechanical tree and stand models, we need to better understand the anchorage of large mature trees. Here, we present a novel dataset to test the following hypotheses: (1) in winching tests, stem deflection has a significant influence on the effectively applied M_a ; (2) M_a for mature conifers can be predicted with simple allometric relationships; (3) the three-dimensional shape and size of the root–soil plate can be predicted with simple allometric relationships; and (4) mature conifers display preferential root growth in the direction of prevailing winds.

Materials and methods

Trees, stand and site

Eighty-four mature trees were winched over in late spring 2000 on a site close to Zürich, Switzerland (47°14' N, 8°53' W) at 460 m a.s.l. The trees included 57 Norway spruces (*Picea abies* L. Karst.), 23 silver firs (*Abies alba* Mill.), and four Scots pines (*Pinus sylvestris* L.), all from the same mixed stand of these species, and some European beech (*Fagus sylvatica* L.) and ash (*Fraxinus excelsior* L.). The forest structure is typical of a managed forest in the Zürich Uplands, the region of the test site. As a result of selective logging, Norway spruce dominates even though it is a natural beech habitat. The density of the mature, single-story stand was about 350 trees ha⁻¹. Although the stand includes local clearings, no test tree grew at the stand edge. Mean cambial age measured at breast height (AGE) of the trees selected for the winching tests was 90 years, the mean tree height (H) was 33 m, and the mean diameter at breast height (DBH) was 46 cm. The distribution of slenderness ($S_n = H/\text{DBH}$) was close to normal, with a mean (\pm SE) of 78 ± 14 . The minimum and maximum values were: DBH = 22 and 70 cm, H = 16 and 42 m, AGE = 46 and 154 years and S_n = 51 and 121, respectively. Among the above-ground coniferous tree parameters, only crown length relative to H differed according to species, with lower values for Scots pine (0.32 ± 0.12) than for Norway spruce (0.49 ± 0.13) and silver fir (0.51 ± 0.11).

The study site has a mean annual precipitation of 1100 mm, a mean temperature of 10 °C and a mean annual wind speed of

1.5 m s⁻¹. The predominant winds blow from the W-WSW sector to E-ENE or vice versa (Schmerlikon weather station, 3 km from the test site; MeteoSwiss 2005). During the period 1900–2000, the site was exposed to several severe storms: 300 times > 20 m s⁻¹, 60 times > 25 m s⁻¹ and 10 times > 30 m s⁻¹ (10-min mean winds; MeteoSwiss 2005). On average and related to the annual harvest, these winds have caused wind-throw to 2% and stem breakage to 0.5% of the conifers in the stand, mainly large trees having been affected (Municipal forester, Blöchli, personal communication, WSL and BUWAL 2001). Soils on the flat test site are medium to deep B-horizons of dystric to gleyic, dystric Cambisols and some Luvisols (taxonomy according to FAO 1998). Throughout the test period, the temperature was above freezing and rainfall was normal for the season.

Test set-up and investigations

The positions of the test trees were first determined with a tachymeter. The trees were then prepared for winching according to a standard test design (e.g., Peltola et al. 2000). A cable was attached at one end to the tree stem at z_a at a relative tree height, $z_{a,\text{rel}} = z_a/H$ (Figure 1). For all trees, $z_{a,\text{rel}}$ was close to normally distributed between 16 to 67%, averaging 39%. The other cable end was wound up by a tractor-driven winch positioned more than one tree height away from the base of the tree. A digital video camera was positioned to capture the deflection of the tree in the winching direction. Before each winching test, the geometry of the winching and recording set-up was measured relative to the stem base, defining the x -axis to be in the winching direction.

The trees were pulled in the E to ENE direction, i.e., in the axis of the prevailing winds and the expected maximum anchorage moment. As the tree was pulled by the cable, the applied cable force (F) and tree deflection were recorded every second (Figure 1). An MTS force sensor (Type 85081-6100-144 V0000C0, 944860, Messtechnik Schaffhausen, Germany)

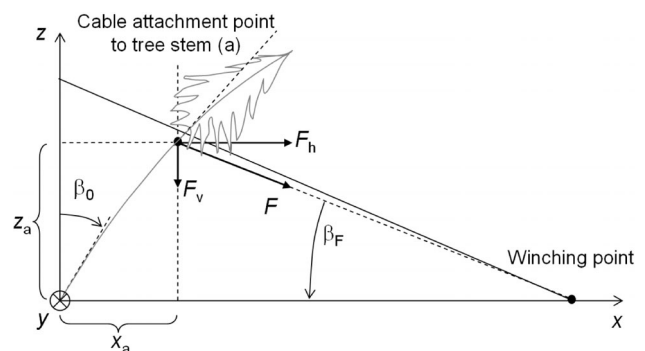


Figure 1. Test set-up for the winching experiments. Abbreviations: β_0 , the stem-base inclination; β_F , the angle of cable-force application; z_a and x_a , the height and the horizontal deflections, respectively, for the point a where the cable is attached to the tree stem; and F_h and F_v , the horizontal and vertical components, respectively, of the winching force F . The inclined continuous line between the tractor and the stem indicates the initial position of the winching cable. All angles occur in the vertical plane $y = 0$.

recorded F , while the stem position was tracked with digital photographs taken approximately perpendicular to the pulling direction. The winching rate was an approximately constant 0.10 m s^{-1} until the tree began to fall under its own weight. In a few cases, it was the stem that failed and not the root–soil system, and a second test was performed with the winch attached to the top of the remaining trunk. All winching tests were performed under near windless conditions. Once the tree was uprooted, we recorded the following measurements and observations of the toppled tree.

Root–soil plate We measured dimensions of the root–soil plate, i.e., the height, width and depth of the overturned, truncated root–soil plate and the plate shape (based on digital photographs of the three main profiles, in the planes $y=0$, $x=0$ and $z=0$). Both dimensions and shape refer to the compact soil of the root–soil plate, ignoring single protruding roots. Wetness (visual determination) of the soil material in the root–soil plate and directly beneath it was classified as waterlogged, moist or dry.

Roots We determined the geometrical distribution and diameter of the roots according to azimuth. The visible occurrence of root rot was noted.

Stem Stem diameter was measured at heights of 0.3, 1.3, 3.0 m, and then every 3 m to the top of the tree. Annual ring width was measured in stem discs cut between the tree base and top.

Crown The mass of branches sampled in 1-m height sections from relative crown heights of 1/8, 3/8, 5/8 and 7/8 was measured with the dynamometer.

The complete dataset (1), including the winching experiment and the parameters recorded from the toppled tree, comprised 75 trees: 52 Norway spruces, 20 silver firs and three Scots pines. Excluding trees affected by root rot from dataset (1) resulted in a dataset (1a) with 61 trees. A reduced dataset (2), excluding data related to the resistive anchorage moment, was obtained for 84 trees: 57 Norway spruces, 23 silver firs and four Scots pines. Excluding trees affected by root rot from (2) resulted in a dataset (2a) with 70 trees: 44 Norway spruces, 22 silver firs and four Scots pines. Only four mature Scots pine trees were available for investigations in the test stand. In the analyses, we used dataset 1 for M_a , 1a for stem deflection and 2a for root–soil plate geometry and root growth.

Turning moment of the root–soil system

In analyzing the mechanics of the root–soil system, we refer to the tree coordinates x , y and z . The line described by the center of the stem intersects with the ground level at $(x,y,z) = (0,0,0)$. The winching force causes displacement of the stem in the plane $y=0$ (Figure 1). To analyze the digital images of stem deflection, we used the software STEMTRACK, which rectifies the images and calculates the deflection of the entire stem in the tree coordinates (x,y,z) for each digital image (every second). The deflection is parameterized by a high-order polynomial $x(z)$. The precision in $x(z)$ depends on the pixel resolution

of the image. We used an image resolution of 768×576 pixels. If a 30-m high tree is captured entirely in one image, one pixel corresponds to ~ 10 cm. With a rectification precision of about 4 cm, the rectification accuracy was higher than the pixel resolution. Technical information on STEMTRACK can be accessed at <http://www.wsl.ch/forschung/forschungsprojekte/Treestability/Stemtrack.pdf> (cited September 28, 2006). All analyses of mechanics and geometry were done with Matlab 7.0 software (MathWorks, USA).

The turning moment applied to the root–soil system (M_o) (Equation 1) was calculated at $(x,y,z) = (0,0,0)$ for every second, from the beginning of the application of the winching force until the tree started to fall under its own weight. From this point, we cannot define values for M_o because our mechanical analysis does not include dynamics and the related forces of inertia. Concerning the point of rotation of the root–soil system, we are aware that it is located at $x > 0$ and presumably $z < 0$, and that $(x,y,z) = (0,0,0)$ is a simplification. Everything belowground is considered as one structural element, namely the “root–soil system,” that resists the M_o .

$$M_o = F \cdot (z_a \cos \beta_F + x_a \sin \beta_F) + \sum_{z=0}^{\text{tree top}} m_{\text{stem}}(z) \cdot g \cdot x(z) + \sum_{\text{crown base}}^{\text{tree top}} m_{\text{branches}}(z) \cdot g \cdot x(z) \quad (1)$$

where the symbols are mostly explained in Figure 1, but $m(z)$ is the mass of the stem and branches, and g is earth gravity (9.82 m s^{-2}). The first term is due to the force application, and the second and third terms are due to gravity. The maximum value of M_o corresponds to the anchorage strength M_a of the tree.

To apply Equation 1, the tree was divided into 100 elements of similar length. Their length was conserved in accordance with the theory of large deflections (e.g., Wood 1995), and the elements diameter and mass of branches m_{branches} (if any) were interpolated (piecewise cubic) from the measured data. The mass of the stem was deduced from the woody stem diameter, bark thickness and the constant moist wood- and bark-bulk density. The bulk density of moist wood was estimated as 825 kg m^{-3} , based on radial growth linked to mass, and that of the bark as 750 kg m^{-3} (Lundström et al. 2007). These estimates are means for all trees and take into consideration the seasonal variations in water content of the stem and the bark (Schmidt-Vogt 1991). The resulting mean bulk density of the stem on bark was 815 kg m^{-3} for a tree of average size, which was used to calculate $m_{\text{stem}}(z)$ for all trees, independent of size.

The contribution to M_o can be divided into three groups, depending on origin: (1) the contribution from F , where only the initial geometry of the winching test is considered; (2) the change in contribution from F caused by the modified geometry, i.e., change in x_a , z_a and β_F (cf. Figure 1); and (3) the contribution from the overhanging tree weight, i.e., gravity. The sum of (1) and (2) is the physically correct contribution from F to M_o , and is thus equal to the first term in Equation 1. To investigate the magnitude of these contributions and to check if the

analysis of M_o (Equation 1) can be simplified, we analyzed the three contributions separately with Equations 2–4, which describe the respective portions of M_o/M_a as:

$$k_{F(\text{ig})} = \frac{F}{M_o} (z_a \cos \beta_F + x_a \sin \beta_F)_{\text{start}} \quad (2)$$

$$k_{\text{geom}} = \frac{F}{M_o} (z_a \cos \beta_F + x_a \sin \beta_F) - k_{F(\text{ig})} \quad (3)$$

$$k_{\text{geom}} = \frac{g}{M_o} \left(\sum_{z=0}^{\text{tree top}} m_{\text{stem}}(z) \cdot x(z) + \sum_{\text{crown base}}^{\text{tree top}} m_{\text{crown}}(z) \cdot x(z) \right) \quad (4)$$

where $k_{F(\text{ig})}$ is the relative contribution to M_o of F , where only the initial geometry (ig) of the tree and the winching test set-up are considered; start is the reference to the initial position of the tree and the winching cable; k_{geom} is the relative contribution to M_o caused by the change in the geometry (geom) of the winching force application compared with at the start of the test; k_{grav} is the relative contribution to M_o from the overhanging tree mass, i.e., gravity (grav); and $k_{F(\text{ig})} + k_{\text{geom}} + k_{\text{grav}} = M_o/M_a = 1.0$.

Geometry of the root–soil plate

The digital photographs of the root–soil plates revealed that a simple fitting of their shapes, such as a cone or a cylinder, would be imprecise. Therefore, we opted for a shape fitted with an ellipse in the plane, and a depth-dependent taper in width and height (Equation 5, Figure 2), where the shape was assumed to be symmetrical along the x - and y -axes. This shape-fitting, which was used to calculate the volume of the root–soil plate (V_{plate} ; Equation 6), concerns the root–soil plate before truncation, which occurred when the tree overturned. The choice of shape fit was a compromise of small errors and a small number of fitting parameters. Mean errors were evaluated for at least ten measurements, randomly distanced along

the profiles in the x - y , x - z and y - z planes (Figure 2). The center of the top of the plate corresponds to $(x,y,z) = (0,0,0)$ of the tree.

$$z_{R,N} = \frac{z_R}{\max(z_R)}$$

$$x_N(z_{R,N}, \phi) = \sin \phi \left(\left(\frac{1 - z_{R,N}}{1 + z_{R,N}} \right)^{nx} - 1 \right)$$

$$y_N(z_{R,N}, \phi) = \cos \phi \left(\left(\frac{1 - z_{R,N}}{1 + z_{R,N}} \right)^{ny} - 1 \right) \quad (5)$$

$$x(z_R, \phi) = x_N(z_{R,N}, \phi) \max(x)$$

$$y(z_R, \phi) = y_N(z_{R,N}, \phi) \max(y)$$

$$V_{\text{plate}} = \pi \int_{z_{R,N}=0}^{z_{R,N}=1} \max(x(z_{R,N})) \max(y(z_{R,N})) dz_R \quad (6)$$

where $z_{R,N}$ is the normalized depth of the root–soil plate, in the range 0–1; z_R is the z -coordinate of the plate, in the range 0– $\max(z_R)$ (m), where $\max(z_R)$ corresponds to $z = 0$ of the tree above ground; $x(z_R, \phi)$ is the dimension of the plate in the x -direction (half height), in the range 0– $\max(x)$ (m); $y(z_R, \phi)$ is the dimension of the plate in the y -direction (half width), in the range 0– $\max(y)$ (m); ϕ is the rotational angle around the z -axis, in the range 0–360° (cf. Figure 2C); and nx, ny are the x - and y -taper of the plate, where $nx, ny < 0.8$ describes a pointed (with tap roots), $0.8 < nx, ny < 2.0$ a rounded, and $nx, ny > 2.0$ a rectangular profile (flat plate, mainly horizontal, lateral roots).

Azimuthal distribution of winds and roots

The distribution of roots with a diameter of 1.0 cm and larger was analyzed according to the azimuth angle θ . The summed

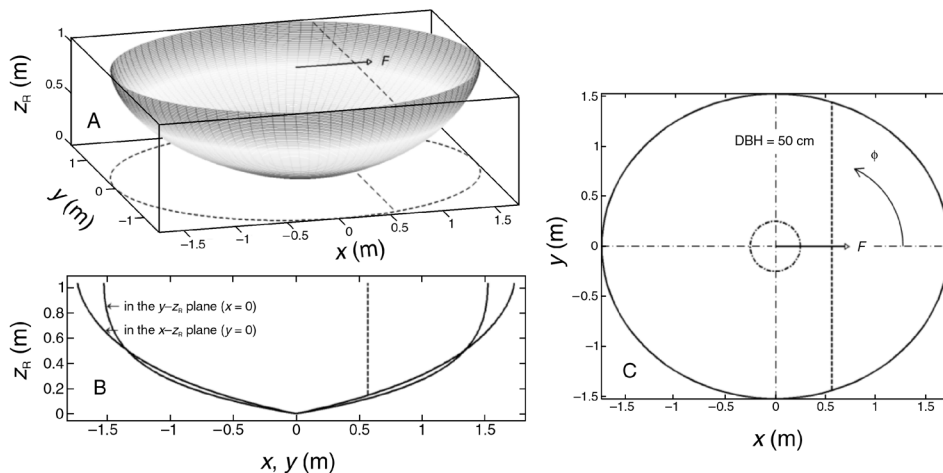


Figure 2. Modeled fit of the root–soil plate in three dimensions (A), with profiles from the side (B) and from above (C). z_R corresponds to the stem centre of the standing tree and x to the stem of the toppled tree, which, in most cases, was also the direction of the winching force (F), and ϕ indicates the rotational angle in the x - y -plane. This example shows a tree with a diameter at breast height (DBH) of 50 cm and x - and y -taper of $nx = 1.4$ (x - z_R -plane) and $ny = 2.0$ (y - z_R -plane), respectively. All straight dashed lines indicate the failure hinge of the root–soil plate at overturning. The remaining, truncated plate is found to the left of this hinge.

cross-sectional area (ΣCSA) of the roots at one fixed radial distance was first determined within 36 azimuthal directions, each having a span of 10° ($0 \pm 5^\circ$, $10 \pm 5^\circ \dots$). This radial distance was selected to be slightly less than the mean radius of the root–soil plate (R_{plate} ; square root of $(\max(x))(\max(y))$; Figure 2) and was consequently different for each tree. The ΣCSA was found to correlate with R_{plate} (cf. Ennos 1993, Bolenikus 2001, Mickovski and Ennos 2003b). To compensate for the relative weighting of large trees on $\Sigma\text{CSA}(\theta)$, ΣCSA within each azimuthal direction was normalized with R_{plate} , resulting in $\Sigma\text{CSA}(\theta)_N$. Thereafter, a mean $\Sigma\text{CSA}(\theta)_N$ was calculated for each of the 36 azimuthal directions. These 36 means were finally normalized with the sum of the 36 means, resulting in $\text{CSA}_{\text{NN}}(\theta)$:

$$\text{CSA}_{\text{NN}}(\theta) = \frac{\text{CSA}_N(\theta)}{\sum_{\theta=0^\circ}^{360^\circ} \text{CSA}_N(\theta)} \quad (7)$$

Roots on the truncated, broken-off part of the root–soil plate were in some cases difficult to assess, because the plates were not always completely overturned (i.e., examined upside down). Therefore, out of a total of 70 investigated plates (dataset 1b), CSA close to the plate hinge was obtained from only 17 plates in the azimuth sector $\text{WSW} \pm 30^\circ$ and from nine plates in the azimuth sector $\text{WSW} \pm 20^\circ$. Finally, the preferential root growth across the entire root–soil plate was calculated as the axis of principal orientation of the 36 CSA_{NN} -vectors, as derived from the Least Squares Orthogonal Distance Fitting.

For wind, we analyzed wind vectors (u) and vectors of wind pressure ($P_w(u)$). The wind vectors were 10-min means measured during 1985–1999 at the Schmerlikon weather station (MeteoSwiss 2005). The wind pressure acting on the undeformed crown was defined as $P_w(u) = c(u)u^2\rho/2$, where ρ is air density = 1.17 kg m^{-3} , with the drag coefficient $c(u) = p + (1 - p)e^{\alpha u}$, where $p = 0.18$ and $\alpha = -0.09$ were from the literature (Johnson et al. 1982, Gardiner et al. 2000, Rudnicki et al. 2004). Azimuthal histograms of $P_w(u)$ were calculated for three classes of wind speed: weak ($1\text{--}6 \text{ m s}^{-1}$), strong ($> 6 \text{ m s}^{-1}$), and all wind speeds $> 0 \text{ m s}^{-1}$ together. The $P_w(u)$ -vector values were counted on circle sector “bins,” with an opening angle of 5° , resulting in 72 directional bins for the speed range of each wind class. The axis of prevailing wind pressure was derived as for the direction of root growth by using the Least Squares Orthogonal Distance Fitting for all $P_w(u)$ -vectors within the three wind-speed classes.

Statistical analysis

The response variables are denoted Y and the explanatory allometric variables X . The Y variables include M_a and the dimensions of the root–soil plate, which were parameterized with the following X variables: DBH, H , total mass of the tree (m_{tree}) and of the stem (m_{stem}), V_{plate} , $\Sigma\text{CSA}(\theta)$ for $0 < \theta < 360^\circ$, R_{plate} , radius of the crown’s projection on the ground (R_{crown}), crown length relative to H and gradient in stem diameter be-

tween 0.3 and 1.3 m tree height. The X variables were selected on the basis of what is easily measurable and on what is commonly used in the literature to enable comparisons with results from published studies.

We first explored the Y variables in multivariate stepwise regression. This analysis yielded regressions of only one significant X , e.g., m_{tree} in the case of M_a . We therefore concentrated on monivariate regressions, including potential combinations and transformations of X variables. The regression equations of M_a were all forced through the origin because a tree with no mass or zero dimensions has an M_a equal to zero. Generally, a regression was considered useful if $R^2 > 0.5$ and a polynomial coefficient was considered meaningful if $P < 0.05$. Significant differences in M_a/X between groups were determined by the Wilcoxon Mann-Whitney Test. This was done for the trees with and without root rot, and with and without stem failure. All differences in allometric relationships between the species were tested similarly.

We use b for regression coefficients, μ for the mean value or the value preceding the standard error ($\pm \text{SE}$) and $\text{SE}_N(Y)$ for the error of predicted value relative to the observed Y value. Levels of significance are denoted as: *, $P < 0.05$; **, $P < 0.01$; ***, $P < 0.001$; and ns, $P > 0.05$.

Results

Influences of stem deflection on the calculated values of M_o and M_a

In all winching experiments, M_o increased first strongly with increasing stem-base inclination (β_o), as expected. The $M_o(\beta_o)$ reached its maximum value, M_a , at a β_o of between 2 and 15° , with a mean value of 5.0° (Figure 3). When this β_o value was exceeded and M_o began to decrease, the roots on the opposite side of the force application were gradually stretched, and, for some trees, these roots even rose vertically in the lateral direction. As these roots failed (in tension, visual observation) at a β_o between about 20 and 30° , the tree began to fall under its own overhanging weight. The overhanging tree weight (k_{grav}) had an important influence on $M_o(\beta_o)$, whereas the change in geometry of the force application (k_{geom}) during the winching experiment influenced $M_o(\beta_o)$ to a lesser extent (Figure 3).

Overhanging tree weight (k_{grav} ; Equation 4) is a result of the overall stem deflection, a combination of stem bending and β_o (Figure 4). Generally, β_o contributed more to k_{grav} than stem bending, apart from a few trees that were winched above half of the tree height. Stem deflection generally increased with winching height and tended to decrease with tree size. The latter resulted from a generally higher β_o at M_a for small trees than for large trees. The minimum value of k_{grav} at M_a was 8% (a silver fir with DBH = 53 cm, $z_{a,\text{start}}/H = 0.20$, $\beta_{F,\text{start}} = 5^\circ$), the maximum value was 42% (a Norway spruce with DBH = 22 cm, $z_{a,\text{start}}/H = 0.55$, $\beta_{F,\text{start}} = 25^\circ$), and the mean value of k_{grav} at M_a was 13%.

The value of k_{geom} (Equation 3) increased with larger winching cable angles at the start of the test $\beta_{F,\text{start}}$ (Figure 1). The point a where the winching cable was attached to the tree stem

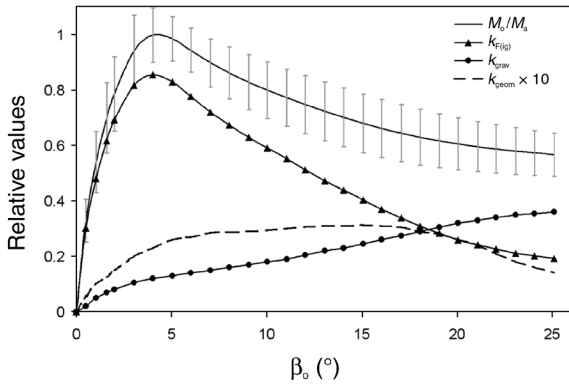


Figure 3. Development of the resistive turning moment of the root–soil system (M_o) with increasing stem-base inclination (β_o) and the relative contributions of the winching force ($k_{F(iig)}$), gravity (k_{grav}) and the geometry of the winching force (k_{geom}) to M_o . When the anchorage strength (M_a) occurs at $\beta_o = 5.0^\circ$, $k_{F(iig)} = 0.84$, $k_{grav} = 0.13$ and $k_{geom} = 0.03$. The curves are the mean values for the investigated trees. Bars indicate the SE of the mean.

described a path, from the test start to M_a , that was close to a circle with a radius equal to the starting winching height ($z_{a,start}$), as shown in Figure 4. Thus, the height coordinate for the force application (z_a) decreased little, whereas the coordinate for the horizontal deflection x_a steadily increased. As a result, the change in β_F from the start of the test to M_a was small, and k_{geom} consequently remained small, even for a $\beta_{F,start}$ value as large as 30° . The minimum value of k_{geom} at M_a was 0% (in general for $\beta_{F,start} < 10^\circ$), the maximum value was 7% (a Norway spruce with DBH = 55 cm $\beta_{F,start} = 29^\circ$), and the mean value of k_{geom} at M_a was 3%.

The value of $k_{F(iig)}$, the part of the actual $M_o(\beta_o)$ that is accounted for if only the initial geometry of the winching test is

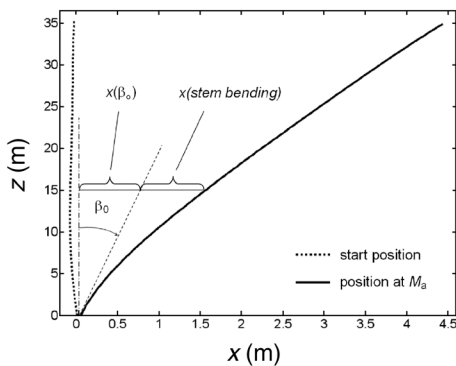


Figure 4. Stem deflection as the applied turning moment of the root–soil system (M_o) reached the anchorage strength (M_a). This silver fir (diameter at breast height = 55 cm, height = 35.2 m), which was not perfectly straight at the start of the test (almost vertical dotted line), was winched at a height of 13.2 m at an angle $\beta_{F,start}$ of 14° . The overhanging tree weight due to stem deflection, originating from the stem-base inclination $x(\beta_o)$ and from stem bending $x(\text{stem bending})$, contributes to M_a . The coordinates of the tree top changed little in z value between the test start and M_a : $(z, x)_{start} = (35.20 \text{ m}, -0.01 \text{ m})$, $(z, x)_{M_a} = (34.91 \text{ m}, 4.44 \text{ m})$.

considered in the analysis of $M_o(\beta_o)$, ranged from 1.0 to 0.30. At M_a , the maximum $k_{F(iig)}$ was 0.90, the minimum was 0.53 and the mean value of $k_{F(iig)}$ at M_a was $1 - \text{mean}(k_{grav}) - \text{mean}(k_{geom}) = 0.84$ (Figure 3).

Values of M_a

Among the 75 Norway spruce, silver fir and Scots pine trees, 13 Norway spruces (25%) and one silver fir (5%) had signs of root rot. These 14 diseased trees were growing in two clusters. Although the roots were not badly attacked in any of the trees, the trees with root-rot displayed 21% lower ($P < 0.05$) M_a/X than the trees without root rot. The M_a of all trees with no root rot was, in turn, best correlated with m_{tree} , m_{stem} , DBH^2H and DBH^2 (Table 1). Trees subjected to a second winching test after stem failure in the first test (19 out of 84 trees) displayed no systematic differences in M_a/X .

For the four regression models, there were no significant differences ($P > 0.5$) in M_a/X between species. This is shown in Figure 5, with M_a as a function of DBH^2H . The other three models in Table 1 displayed similar scattering of the M_a data. In Figure 5, we comment on two outliers labeled 1 and 2. The root system of the first outlier (1), a Norway spruce (DBH = 25 cm, $S_n = 121$), was, unlike that of other trees, firmly interlocked with the root–soil system of another close neighbor spruce of DBH = 24 cm, and both trees were overturned together during the winching test. This tree was excluded from all statistical analyses. A very large proportion of the lateral roots of the second outlier (2), also a Norway spruce (DBH = 46 cm, $S_n = 70$), was pulled laterally up above the ground over

Table 1. Statistical data related to models describing the anchorage strength ($M_a = bX$ (kN m) based on 38 Norway spruces, 19 silver firs and three Scots pines. Only trees without root rot were considered. Abbreviations: m_{tree} and m_{stem} (kg), the total mass of the tree and of the stem, respectively; DBH (m), the stem diameter at breast height; and H (m), the tree height. The models are listed top-down according to the quality (R^2) of the models including all (All) three species.

X	Species	b	SE(p)	SE _N (M_a)	R^2
m_{tree}	Spruce	1.25E-1 ***	4.1E-3	0.18	0.76
	Fir	1.20E-1 ***	4.9E-3	0.18	0.82
	Pine	1.23E-1 ***	2.1E-3	0.02	0.98
	All	1.22E-1 ***	2.9E-3	0.17	0.81
m_{stem}	Spruce	1.62E-1 ***	5.5E-3	0.18	0.73
	Fir	1.73E-1 ***	8.3E-3	0.20	0.75
	Pine	1.57E-1 *	1.8E-2	0.14	0.01
	All	1.66E-1 ***	4.5E-3	0.19	0.76
DBH^2H	Spruce	4.19E+1 ***	1.4	0.20	0.76
	Fir	4.15E+1 ***	2.2	0.20	0.71
	Pine	4.18E+1 *	5.1	0.15	-0.14
	All	4.17E+1 ***	1.1	0.20	0.76
DBH^2	Spruce	1.48E+3 ***	5.1E+1	0.20	0.73
	Fir	1.46E+3 ***	8.5E+1	0.21	0.64
	Pine	1.47E+3 *	2.1E+2	0.15	-0.51
	All	1.47E+3 ***	4.3E+1	0.20	0.71

a long distance as the tree turned over.

Characteristics of the root–soil plate

The correlations between dimensions of the root–soil plate and aboveground tree parameters were weak. This also applies to the relationships between width (twice the maximum y -value, Figure 2), height (twice the maximum x -value) and depth (the maximum z -value) of the individual root–soil plates. Consequently, the corresponding regression models provided a poor fit to the data (Table 2). The respective R^2 values were in all cases highest with DBH as the explanatory variable, apart from V_{plate} , which was best described by DBH^2H . The soil in the root–soil plate and directly beneath it was generally dry to slightly moist.

The taper of the root–soil plate n_y tended to be greater than n_x , typically $n_y = 2.0$ and $n_x = 1.4$ (Figure 2). However, the depth taper displayed large variations ($\text{SE} = 0.8$, $\text{min} = 0.4$, $\text{max} = 3.2$) with no obvious pattern. As the root–soil plate fit was adapted to each plate individually, the overall mean errors in profile and volume were small ($\text{SE}_N < 0.10$, $\text{SE}_N < 0.12$), and mainly caused by departures from the elliptic fit of the cross section (in the x – y plane). The truncation (broken-off part) of the root–soil plate on the pulling side (positive x -side) due to pressure from the tree mass when the tree toppled, was slightly more than half of the maximum x -value in this direction (Figures 2B and 2C).

Azimuthal distribution of roots and wind

The directions of root growth and wind display affinities. The preferential axis of the mean distribution of root CSA (Figure 6A) was close to the prevailing axis of wind pressure (Figure 6B). The separate considerations of weak and strong winds show that the root system adapts more to frequent winds of low magnitude than to the less frequent storms, though the differences were small. The azimuthal directions θ for the axis of preferential root growth and wind did not differ with weak winds, whereas with strong and less frequent winds, the differ-

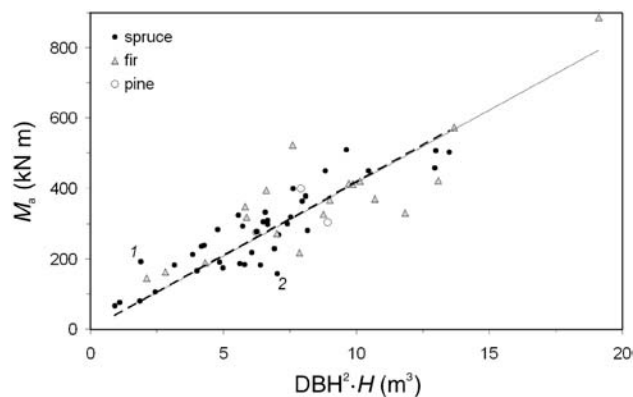


Figure 5. Anchorage strength (M_a) for trees with no root rot plotted against stem diameter at breast height squared times tree height (DBH^2H). The regressions for Norway spruce (fine continuous line), silver fir (hatched line) and Scots pine (not displayed, because it was between those of the Norway spruce and silver fir) are almost identical. Two outliers are indicated (1 and 2).

ence was 8° . If all magnitudes of winds were considered together, the difference was 4° .

Discussion

Influence of stem deflection on the calculated value of M_a

Stem deflection occurs as a tree is pushed by lateral forces, which may be either artificial (e.g., pulled by a winch) or natural (e.g., wind). In either case, the overhanging tree weight contributes to the effectively applied turning moment of the root–soil system. In addition, the stem deflection that occurs during a winching test typically modifies the geometry of the force application.

Stem deflection results from stem bending and rotation of the root–soil system β_o . We compared our β_o and k_{grav} values with those in the literature (Table 3). Most of the latter values refer, however, to the stem position at maximum force application and not to that at M_a . Our winching experiments showed that both β_o and k_{grav} were up to 25% lower at maximum force application than at M_a . They also showed that k_{grav} increased substantially if F was applied above $z_{\text{rel}} = 0.5$. It is apparent that both stem-base inclination and stem bending need to be considered when calculating M_a from winching tests. A thorough comparison of $\beta_o(M_a)$ and k_{grav} requires reference to the same type of stem-base moment, i.e., that M_a systematically accounts for the overhanging tree weight. Compared with k_{grav} , k_{geom} is of minor importance in the analysis of the resistive turning moment of the root–soil system. However, under special winching conditions (e.g., for trees winched on a slope), it is possible that k_{geom} becomes more relevant.

Because of the complexity of stem deflection mechanics, it seems impossible to describe the contributions of k_{grav} and k_{geom} to M_a with simple allometric models. Hence, when calculating M_a from winching tests, these contributions need to be determined experimentally. We suggest stem deflection be re-

Table 2. Response variable (Y) and explanatory variables (X) related to the root–soil plate. All regressions include all 70 Norway spruce, silver fir and Scots pine trees. All regression coefficients (b) are significant at $P < 0.001$.

Y	X	b	$\text{SE}(b)$	$\text{SE}_N(Y)$	R^2
Width	DBH	5.9	0.19	0.26	0.19
Height	DBH	6.6	0.23	0.30	0.11
Depth	DBH	2.0	0.07	0.35	0.08
R_{plate}	DBH	3.1	0.09	0.24	0.19
V_{plate}^a	DBH^2H	0.45	0.03	0.53	0.28
Height ^b	Width	1.1	0.04	0.23	0.24
Depth ^c	Width	0.32	0.01	0.38	0.04

^a Compared with Norway spruce, b was 27% larger ($P < 0.05$) for silver fir and 35% larger ($P > 0.05$) for Scots pine.

^b $b = 1.20$ (Norway spruce); 1.13 (silver fir); 1.29 (Scots pine), but the differences were not significant.

^c The differences in b were negligible ($< 3\%$) between Norway spruce, silver fir and Scots pine.

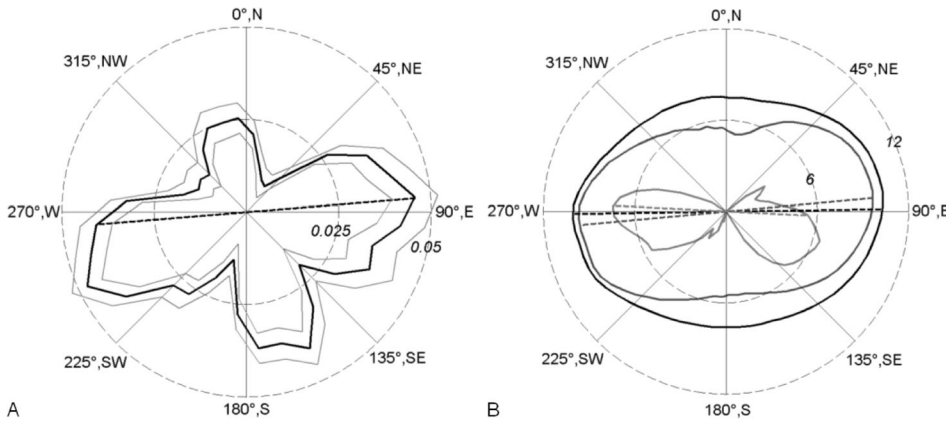


Figure 6. Direction of (A) root growth compared with that of (B) wind. (A) The average distribution of normalized cross sectional area (CSA) of roots according to azimuth angle (θ) displayed by one circle histogram (continuous black line; gray line is the SE), with the axis of principal orientation of CSA at $\theta = 265^\circ/85^\circ$ (black dashed line). (B) The direction of wind pressure on the tree depending on the magnitude of wind speed (u), displayed by three separate circle histograms (continuous lines). The

axes of principal orientations of wind pressure are: for all wind data $u > 0 \text{ m s}^{-1}$ (the black and outermost line) at $\beta = 269^\circ/89^\circ$ (dashed), for low wind-speed data $1 < u < 6 \text{ m s}^{-1}$ (dark gray line) at $\beta = 265^\circ/85^\circ$, and for high wind-speed data $u > 6 \text{ m s}^{-1}$ (light gray and innermost line) at $\beta = 273^\circ/93^\circ$. The radial graduation corresponds to $\log(\text{number of data per bin})$.

Table 3. Comparison of the stem-base inclination (β_o) as the anchorage strength (M_a) is reached and the contribution of the overhanging tree weight (k_{grav}) to M_a . Abbreviations: AGE, mean cambial age measured at breast height; DBH, stem diameter at breast height; and z_{rel} , the relative tree height.

Species	Soil B-Horizon	Forest stand: Density, type	AGE	DBH	z_{rel}	$\beta_o(M_a)$	k_{grav}	Reference
			min-max mean (year)	min-max mean (cm)	min-max mean	min-max mean ($^\circ$)	min-max mean (%)	
<i>Picea abies</i> <i>Abies alba</i> <i>Pinus sylvestris</i>	Cambisols, luvisols	350, co-dominant	46–154 ¹ 90 ¹	22–70 46	0.16–0.67 0.39	2–15 ² 5 ²	8–42 ² 13 ²	This study
<i>Picea sitchensis</i>	Shallow peaty gley	co-dominant	34 34	19–23 21	– 0.18	1–10 ^{3,4} 4 ³	– –	Coutts (1983)
<i>Picea sitchensis</i>	Shallow peaty gley	4000 ha ⁻¹ , co-dominant	35 35	15–27 20	– 0.73	1–10 ^{3,4} 26 ^{2,4}	60–70 ² 67 ²	Coutts (1986)
<i>Picea sitchensis</i>	Shallow peaty gley	4000 ha ⁻¹ , co-dominant	20–50 –	10–35 –	– –	– –	– 22 ³	Gardiner et al. (2000)
<i>Picea sitchensis</i>	Shallow peaty gley	4000 ha ⁻¹ , co-dominant	– 40	– 23	– 0.5	– –	– 14 ³	Achim et al. (2003)
<i>Pinus taeda</i>	Fine sand	1000 ha ⁻¹	– 30	13–41 –	– 0.5	2–35 ^{1,3} 6 ^{1,3}	– –	Fredericksen et al. (1993)
<i>Pinus sylvestris</i>	Sandy, silty podzol	1000–1800 ha ⁻¹	40–100 –	14–23 –	0.3–0.5 –	– –	5–20 ³ –	Peltola (1995), Peltola et al. (2000)
<i>Pinus radiata</i>	Shallow, compact gravel	–	10–39 –	23–52 –	0.2–0.4 –	– –	– 9 ³	Papesch et al. (1997)
<i>Pinus pinaster</i>	Sandy podzol	100–1000 ha ⁻¹	15–50 –	18–41 –	0.1–0.5 –	– –	4–14 ³ 9 ³	Cucchi et al. (2004)

¹ Measured at breast height.

² At maximum stem-base moment.

³ At maximum force application.

⁴ Of the root–soil plate, β_o at the stem base ought to be greater because roots deform and bend more easily than the relatively rigid stem base.

corded as a function of stem height, e.g., according to the methods we used.

Allometric predictions of M_a

The M_a was well predicted by either tree mass, stem mass (or stem volume), DBH^2H , or DBH^2 (listed in order of R^2). This is in line with results obtained for Scots pine, Norway spruce and birch (Peltola et al. 2000, Bolenikus 2001), white spruce and balsam fir (Meunier et al. 2002) and silver fir (Stokes et al. 2005). The M_a -model ranking shows that tree anchorage is better adapted to the size of the tree (crown and stem) than to the cross-sectional area at the stem base. Including belowground tree variables (e.g., root CSA or the dimensions of the root-soil plate) in the retained M_a -models of aboveground variables did not improve the quality of the models, in contrast to previous studies on tree anchorage (Papesch et al. 1997, Peltola et al. 2000, Mickovski and Ennos 2003b, Cucchi et al. 2004).

For the trees without root rot, we compared our $M_a/(DBH^2H)$ and M_a/m_{stem} data with published values (Table 4). Although our regression coefficients are close to the values in the literature, our coefficients are among the largest. We offer four explanations for this discrepancy: (1) not all

studies included k_{grav} and k_{geom} ; (2) only our M_a values were derived from winching in the direction of prevailing winds, and were thus likely to be the largest M_a values in terms of azimuth (Danjon et al. 2005); (3) our experiments were conducted on relatively deep and generally well-drained soils; and (4) only our M_a values refer to the tree position at the maximum effective stem-base moment M_a , whereas the M_a values in other studies refer to the position at maximum force application.

The lack of significant differences in M_a/X between Norway spruce and silver fir for trees without root rot is probably associated with local growth conditions: when growing in a mixed stand, both species are limited by similar growth conditions, resulting in a growth response independent of species (Polomski and Kuhn 1998). Therefore, inhibition of root system growth typical of the species is more probable with increasing tree size (Köstler et al. 1968). It is likely that more intensive examinations of local soil and growth conditions would have helped explain more of the overall variations in M_a , and possibly also to explain why no differences were found between the species in the mixed forest. The number of Scots pine trees studied (four) is too low to test whether it differs significantly from silver fir and Norway spruce in any of the anchorage properties studied. Because of root rot, Norway

Table 4. Comparison of M_a -regression coefficients, M_a/m_{stem} and $M_a/(DBH^2H)$. Abbreviations: AGE, mean cambial age measured at breast height; DBH, stem diameter at breast height; M_a , the maximum resistive turning moment; m_{stem} , the mass of the stem; H , tree height; k_{grav} , the relative contribution to M_o from the overhanging tree mass; k_{geom} , the relative contribution to M_o caused by the change in geometry of the winching force application compared with at the start of the test; and M_o , the turning moment applied to the root-soil system.

Species	Soil B-Horizon	Forest stand	AGE (years)	DBH (cm)	M_a/m_{stem} (kN m kg ⁻¹)	$M_a/(DBH^2H)$ (kN m m ⁻³)	Inclusion of k_{grav} ; k_{geom}	Reference
<i>Picea abies</i>	Cambisols, luvisols	350 ha ⁻¹	46–154	22–70	0.16	42	Yes; Yes	This study
<i>Abies alba</i>					0.17	42		
<i>Pinus sylvestris</i>					0.16	42		
<i>Picea sitchensis</i>	Peaty gley Shallow brown Deep brown	Dense plantation	30	21	0.12 0.17 0.21	–	Yes; Yes	Fraser and Gardiner (1967)
<i>Picea sitchensis</i>	“Free draining brown”	Dense plantation	40	23	0.11 ¹ 0.10 ¹ 0.086 ¹	–	Yes; Yes	Achim et al. (2003)
<i>Picea sitchensis</i>	Peaty, surface water gley	4000 ha ⁻¹	46	32	0.04–0.14 ²	–	No; No	Ray and Nicoll (1998)
<i>Pinus sylvestris</i>	Sandy, silty podzol	1300–1800 ha ⁻¹	40–100	14–23	0.13 ³	36	No; Yes	Peltola et al. (2000)
<i>Picea abies</i>	Sandy, silty podzol	1000–1600 ha ⁻¹	80–100	16–23	0.11 ³	33	No; Yes	Peltola et al. (2000)
<i>Pinus pinaster</i>	Sandy podzol	100–1000 ha ⁻¹	15–50	18–41	–	35 ⁴ 45 ⁴ 40 ⁴	Yes; Yes	Cucchi et al. (2004)

¹ When pulled down slope/across slope/upslope.

² Higher values with deeper water table.

³ Derived by Gardiner et al. (2000) from the experiments of Peltola et al. (2000).

⁴ The regressions were not forced through zero, but the intercept values were small. The three values refer to: trees on soil with a hard pan within the stand; trees on the stand edge; and trees within the stand on soil with no hard pan.

spruce had significantly weaker root–soil anchorage than the other species in the test area.

Shape of the root–soil plate and allometric predictions of its size

The shape of the root–soil plate was well described with a depth-dependent taper model with an elliptical cross section. We compared the performance of this fit to calculate the total plate volume (based on mean values of nx , ny and $\max(x)/\max(y)$) with that of two other fits: a circular-conical shape (Peltola and Kellomäki 1993) and an elliptical cross section, but with a constant profile in depth (Cucchi et al. 2004) similar to the profiles used by Blackwell et al. (1990) and Coutts (1983). Considering the individually fitted plates (Equation 5) as reference volumes, we obtained min/mean/max errors of $-25/-5/+70\%$ for the taper model, $-110/-40/+10\%$ for the circular-conical fit and $+20/+50/+560\%$ for the ellipsoidal fit. Thus, the averaged taper model seems to yield good predictions of shape and volume.

The dimensions of the root–soil plate exhibited larger intra-species differences than interspecies differences, which corresponds with the findings of Brang and Bachofen (2002). The horizontal and vertical plate size was weakly correlated with DBH, similar to the Norway spruce and Scots pine analyzed by Hakkila (1972). The shape and dimensions of the root–soil plate are largely governed by root architecture (Danjon et al. 2005). We therefore believe that the same masking effects described for M_a help explain both the lack of significant differences between species in root–soil plate dimensions and the weak allometric relationships within species.

As the trees toppled, the root–soil plate failed at a distance from the stem center that was less than 50% of the root–soil plate radius in the winching direction ($< 0.5\max(x)$; cf. Figure 2), similar to the $0.4\max(x)$ obtained for Sitka spruce planted close to furrows (Coutts 1983, Ray and Nicoll 1998). The broken-off part of the root–soil plate represented 20–30% of the total (modeled) volume of the root–soil plate of the standing tree.

Azimuthal direction of root growth related to prevailing winds

The distribution of the cross-sectional root area (CSA) was, on average, concentrated in the prevailing wind axis. This confirms the claim that mature trees adapt their root growth to the orientation of prevailing winds, just as do young trees (Nicoll and Ray 1996). The roots seem to adapt their azimuthal CSA more to weak and frequent winds than to rare and heavy storms, although the differences are small. Because maximal M_a is considered to coincide with the axis of preferential orientation of coarse roots (e.g., Coutts 1986, Nicoll and Ray 1996), we consider that our trees were tested in the azimuth of their maximum M_a .

We reached four conclusions from our study. (1) In winching tests, stem bending and the rotation of the root–soil system have a significant influence on the effectively applied M_a . We propose recording stem deflection as a function of tree height

when M_a is calculated from winching tests. (2) The M_a for mature conifers can be accurately predicted by monovariate regression with either tree mass, stem mass, DBH^2H or DBH^2 . (3) The three-dimensional shape and size of the root–soil plate were weakly correlated with all allometric parameters. (4) Mature conifers showed preferential root growth in the direction of frequent low wind events.

Acknowledgments

We thank the Board of the Swiss Federal Institutes of Technology for financial support as part of the “Tree Stability and Natural Hazards” (“Naturereignisse und Baumstabilität”) project, M. Ammann, F. Michel and L. Lorenzato for field assistance, P. Lüscher for soil data, MeteoSwiss for climate data and S. Dingwall for revision of the text.

References

- Achim, A., B.C. Nicoll, S. Mochan and B.A. Gardiner. 2003. Wind stability of trees on slopes. *In* Wind Effects on Trees. Eds. B. Ruck, C. Kottmeier, C. Mattheck, C. Quine and G. Wilhelm. University of Karlsruhe, Karlsruhe, Germany, pp 231–237.
- Blackwell, P.G., K. Rennolls and M.P. Coutts. 1990. A root anchorage model for shallowly rooted Sitka spruce. *Forestry* 63:73–92.
- Bolenikus, D. 2001. Zur Wurzel Ausbildung von Fichte (*Picea abies* L. Karst) und Weisstanne (*Abies alba* Mill.) in gleich- und ungleichaltrigen Beständen. *Ber. Freiburger Forstl. Forsch.* 35:155.
- Brang, P. and H. Bachofen. 2002. Kleiner Wurzelballen—grosser Lotharschaden? *Inf.bl. Forsch.bereich Wald* 11:3.
- Brassel, P. and U.-B. Brändli. 1999. Inventaire forestier national Suisse. Résultats du deuxième inventaire 1993–1995. Haupt, Berne, 442 p.
- Coutts, M.P. 1983. Root architecture and tree stability. *Plant Soil* 71:171–188.
- Coutts, M.P. 1986. Components of tree stability in Sitka spruce on peaty gley soil. *Forestry* 59:173–198.
- Coutts, M.P., C.C.N. Nielsen and B.C. Nicoll. 1999. The development of symmetry, rigidity and anchorage in the structural root system of conifers. *Plant Soil* 217:1–15.
- Crook, M.J. and A.R. Ennos. 1996. The anchorage mechanics of deep rooted larch, *Larix europea* \times *L. japonica*. *J. Exp. Bot.* 47: 1509–1517.
- Cucchi, V., C. Meredieu, A. Stokes, S. Berthier, D. Bert, M. Najjar, A. Denis and R. Lastennet. 2004. Root anchorage of inner and edge trees in stands of Maritime pine (*Pinus pinaster* Ait.) growing in different podzolic soil conditions. *Trees* 18:460–466.
- Danjon, F., T. Fourcaud and D. Bert. 2005. Root architecture and wind-firmness of mature *Pinus pinaster*. *New Phytol.* 168: 387–400.
- Dupuy, L., T. Fourcaud and A. Stokes. 2005. A numerical investigation into the influence of soil type and root architecture on tree anchorage. *Plant Soil* 278:119–134.
- Ennos, A.R. 1993. The scaling of root anchorage. *J. Theor. Biol.* 161:61–75.
- FAO. 1998. Soil map of the world. Revised legend. World soil resources report Vol. 60. FAO-Unesco, Food and Agriculture Org. of the United Nations, Rome, 119 p.
- Fourcaud, T., F. Blaise, P. Lac, P. Castera and P. de Reffye. 2003a. Numerical modeling of shape regulation and growth stresses in trees II. Implementation in the AMAPpara software and simulation of tree growth. *Trees* 17:31–39.

- Fourcaud, T., F. Danjon and L. Dupuy 2003b. Numerical analysis of the anchorage of maritime pine trees in connection with root structure. *In* Wind Effects on Trees. Eds. B. Ruck, C. Kottmeier, C. Mattheck, C. Quine and G. Wilhelm. University of Karlsruhe, Karlsruhe, Germany, pp 323–330.
- Fraser, A.I. 1962. The soil and roots as factors in tree stability. *Forestry* 35:117–127.
- Fraser, A.I. and J.B.H. Gardiner. 1967. Rooting and stability in Sitka spruce. *For. Comm. Bull. Vol. 40.* HMSO, London, 28 p.
- Fredericksen, T.S., R.L. Hedden and S.A. Williams. 1993. Testing Loblolly-pine wind firmness with simulated wind stress. *Can. J. For. Res.* 23:1760–1765.
- Gardiner, B.A., H. Peltola and S. Kellomäki. 2000. Comparison of two models for predicting the critical wind speeds required to damage coniferous trees. *Ecol. Model.* 129:1–23.
- Hakkila, P. 1972. Mechanized harvesting of stumps and roots. *Communicationes Instituti Forestalis Fenniae. Communicationes Instituti Forestalis Fenniae* 77:1, Helsinki, 71 p.
- Johnson, R.C., G.E. Ramey and D.S. Ohagan. 1982. Wind induced forces on trees. *J. Fluids Eng.-Trans. ASME* 104:25–30.
- Jonsson, M.J., A. Foetzi, M. Kalberer, T. Lundström, W. Ammann and V. Stöckli. 2006. Root–soil rotation stiffness of Norway spruce (*Picea abies* L. Karst.) growing on subalpine forested slopes. *Plant Soil* 285:267–277.
- Köstler, J.N., E. Brückner and H. Bibelriether. 1968. Die Wurzeln der Waldbäume. Vol. III. Verlag Paul Parey, Hamburg Berlin, 284 p.
- Lundström, T., U. Heiz, M. Stoffel and V. Stöckli. 2007. Fresh wood bending: linking properties of mechanics and growth within the stem. *Tree Physiol.* 27:1229–1241.
- Mattheck, C., K. Bethge and D. Erb. 1993. Failure criteria for trees. *Allg. Forst Jagdztg.* 164:9–12.
- MeteoSwiss. 2005. Climate database. Swiss National Weather Service. http://www.meteoschweiz.ch/web/en/services/data_portal.html.
- Meunier, S., J.C. Ruel, G. Laflamme and A. Achim. 2002. Comparative resistance of white spruce and balsam fir to overturning. *Can. J. For. Res.* 32:642–652.
- Mickovski, S.B. and A.R. Ennos. 2003a. The effect of unidirectional stem flexing on shoot and root morphology and architecture in young *Pinus sylvestris* trees. *Can. J. For. Res.* 33:2202–2209.
- Mickovski, S.B. and A.R. Ennos. 2003b. Anchorage and asymmetry in the root system of *Pinus peuce*. *Silva Fenn.* 37:161–173.
- Milne, R. and P. Blackburn. 1989. The elasticity and vertical distribution of stress within stems of *Picea sitchensis*. *Tree Physiol.* 5:195–205.
- Moore, J.R. 2000. Differences in maximum resistive bending moments of *Pinus radiata* trees grown on a range of soil types. *For. Ecol. Manage.* 135:63–71.
- Nicoll, B.C. and D. Ray. 1996. Adaptive growth of tree root systems in response to wind action and site conditions. *Tree Physiol.* 16: 891–898.
- Nicoll, B.C., E.P. Easton, A.D. Milner, C. Walker and M.P. Coutts. 1995. Wind stability factors in tree selection: distribution of biomass within root systems of Sitka spruce clones. *In* Wind and Trees. Eds. M.P. Coutts and J. Grace. Cambridge University Press, Cambridge, pp 276–292.
- Nicoll, B.C., A. Achim, S. Mochan and B.A. Gardiner. 2005. Does steep terrain influence tree stability? A field investigation. *Can. J. For. Res.* 35:2360–2367.
- Nicoll, B.C., B.A. Gardiner, B. Rayner and A.J. Peace. 2006. Anchorage of coniferous trees in relation to species, soil type, and rooting depth. *Can. J. For. Res.* 36:1871–1883.
- Papesch, A.J.G., J.R. Moore and A.E. Hawke. 1997. Mechanical stability of *Pinus radiata* trees at eyrewell forest investigated using static tests. *N.Z. J. For. Sci.* 27:188–204.
- Peltola, H. 1995. Studies on the mechanism of wind-induced damage of Scots pine. *Research Notes of the Faculty of Forests* 32, University of Joensuu, 28 p.
- Peltola, H. and S. Kellomäki. 1993. A mechanistic model for calculating windthrow and stem breakage of Scots pine at stand edge. *Silva Fenn.* 27:99–111.
- Peltola, H., S. Kellomäki, A. Hassinen and M. Granander. 2000. Mechanical stability of Scots pine, Norway spruce and birch: an analysis of tree-pulling experiments in Finland. *For. Ecol. Manage.* 135:143–153.
- Polomski, J. and N. Kuhn. 1998. Wurzelsysteme. Haupt Verlag, Bern, 290 p.
- Ray, D. and B.C. Nicoll. 1998. The effect of soil water-table depth on root-plate development and stability of Sitka spruce. *Forestry* 71:169–182.
- Rudnicki, M., S.J. Mitchell and M.D. Novak. 2004. Wind tunnel measurements of crown streamlining and drag relationships for three conifer species. *Can. J. For. Res.* 34:666–676.
- Schiesser, H.H., C. Pfister and J. Bader. 1997. Winter storms in Switzerland north of the Alps 1864/1865-1993/1994. *Theor. Appl. Climatol.* 58:1–19.
- Schmidt-Vogt, H. 1991. Die Fichte: ein Handbuch in zwei Bänden. Waldbau, Ökologie, Urwald, Wirtschaftswald, Ernährung, Düngung, Ausblick Vol. 2/3. Verlag Paul Parey, Hamburg, 781 p.
- Stokes, A., A.H. Fitter and M.P. Coutts. 1995. Responses of young trees to wind and shading—effects on root architecture. *J. Exp. Bot.* 46:1139–1146.
- Stokes, A., F. Salin, A.D. Kokutse et al. 2005. Mechanical resistance of different tree species to rockfall in the French Alps. *Plant Soil* 278:107–117.
- Wessolly, L. and M. Erb. 1998. Handbuch der Baumstatik und Baumkontrolle. Patzer, Berlin, 270 p.
- Wood, C.J. 1995. Understanding wind forces on trees. *In* Wind and Trees. Eds. M.P. Coutts and J. Grace. Cambridge University Press, Cambridge, pp 133–164.
- WSL and BUWAL. 2001. Lothar der Orkan 1999 Ereignisanalyse. Eidg. Forschungsanstalt WSL, Bundesamt für Umwelt, Wald und Landschaft BUWAL, Birmensdorf, Bern, 365 p.
- Yang, Y.B., Y.T. Yang and H.H. Su. 2005. Behavior of the tree branches, trunk, and root anchorage by nonlinear finite element analysis. *Adv. Struct. Engineer.* 8:1–14.